The Ejecta Structure of the O-rich SNR Puppis A revealed by XMM-Newton

Satoru KATSUDA (Osaka U.), Koji MORI (Miyazaki U.), Hiroshi TSUNEMI (Osaka U.), Sangwook PARK (PSU), Una HWANG (NASA/GSFC), David N. BURROWS (PSU), Patrick O. SLANE (CfA), John P. HUGHES (Rutgers U.)

Introduction & Observations

Puppis A is a middle aged (~4000 years; Blair et al. 2005) X-ray bright supernova remnant (SNR). Optical spectroscopy (Winkler & Kirshner 1985) revealed fast moving knots (FMKs) of O-rich material in the northeastern portion of Puppis A, leading to the classification of the SNR as "oxygen-rich". Near the geometric center of Puppis A is a central compact object (CCO) (Petre et al. 1996), whose proper motion was recently measured to be 1200~1500 km/sec toward the southwest (Winkler & Petre 2006; Hui & Becker 2006), opposite to the direction of motion of the O-rich FMKs. The motions of the CCO and FMKs are generally consistent with a common site for a supernova (SN) explosion occurring some 3000-4000 years ago. In addition to the O-rich FMKs, recent Suzaku observations have revealed evidence for Si-S-rich material near the northeastern rim (Hwang et al. 2006). Establishing links between SN ejecta and a compact stellar remnant is a key step for understanding SN explosion mechanisms (e.g., Scheck et al. 2006). Puppis A is an ideal target for investigating such links.

Puppis A has been observed 5 times with XMM-Newton from 2001 to 2005. Here we report results from spatially resolved spectral analysis using all the XMM-Newton data.

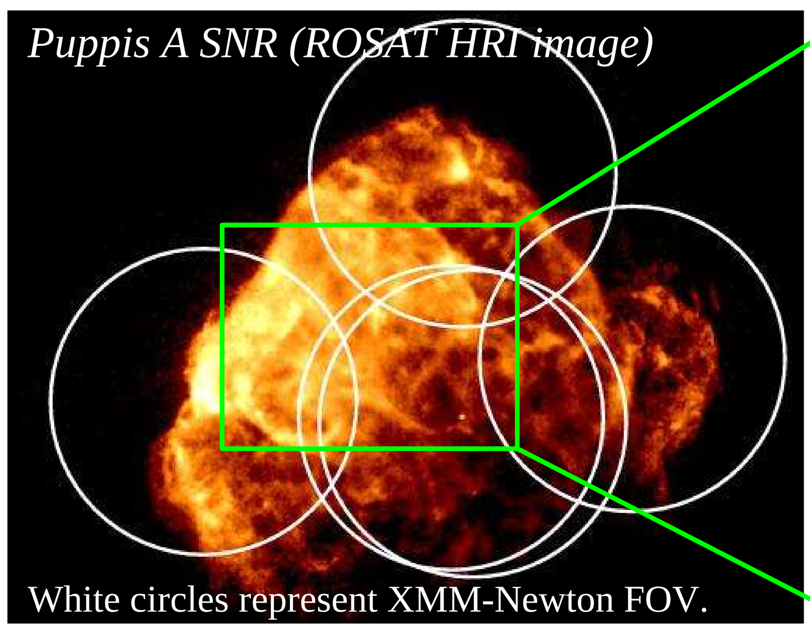

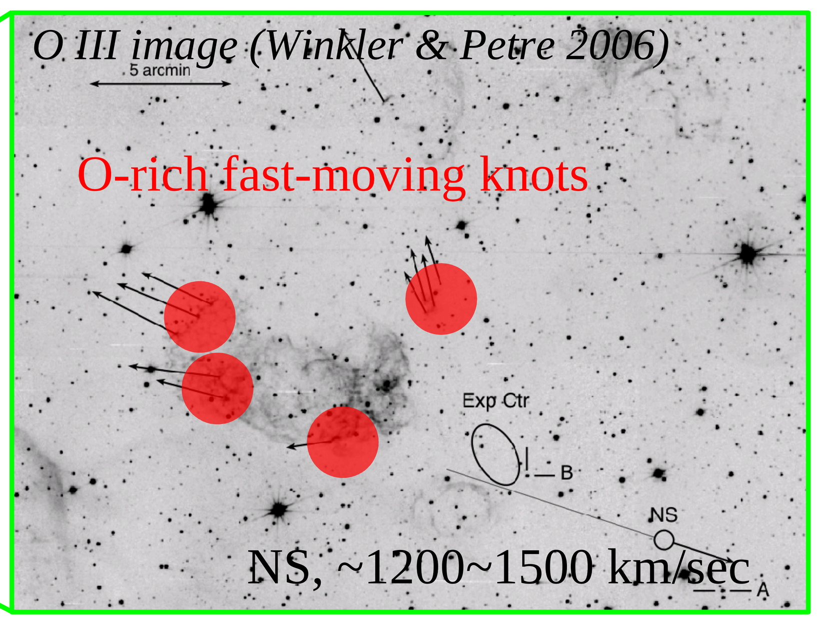

Spatially Resolved Spectral Analysis

- One-kTe component model fitting

A three color image of merged MOS1/2 and PN data from all five XMM-Newton observations is shown below. The stripe of blue-colored emission (with an apparently harder X-ray spectra) extending through the remnant from the northeast to south-west is believed to be due to increased absorption of soft X-rays by excess foreground material (Arendt et al. 1990; Aschenbach 1993). We divided the entire FOV into small rectangular cells so that each cell (see figure below) contained a similar number of photons (50,000-100,000 for MOS1+MOS2+PN). Then we extracted a spectrum from each cell and performed X-ray spectral analysis. Initially, we applied a one-kTe component non-equilibrium ionization (NEI) model. Free parameters are absorption column, N_H; electron temperature, kTe; ionization time, τ; emission measure, EM (EM=$\int n_e n_H dl$, dl is the plasma depth); and abundances of O(=C=N), Ne, Mg, Si, S, and Fe(=Ni). The reduced χ^2 map is shown below.

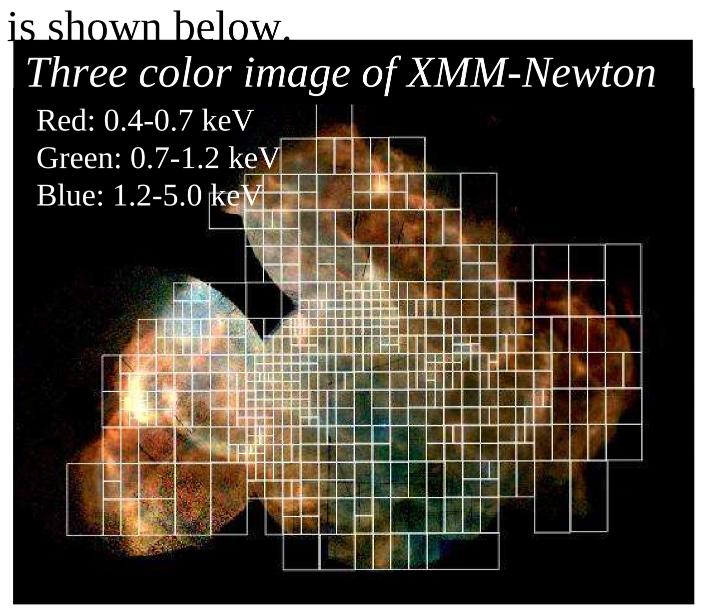

Reduced χ^2 map

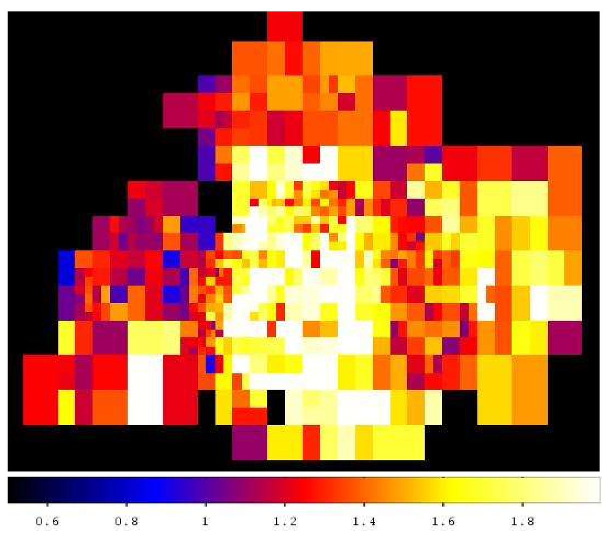

- Abundances in Rim Regions (ISM abundances)

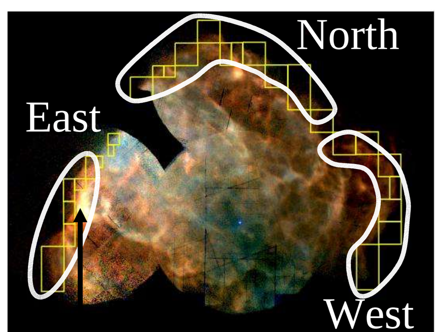

Based on the reduced χ^2 map, we see that spectra from the rim regions are relatively well represented by this initial model, while those from the central portion are less so. Below, we show example spectra from a cell in the rim regions and present a summary of mean abundances in the eastern, northern, and western rims (which are indicated as white lines in the left figure) with mean errors.

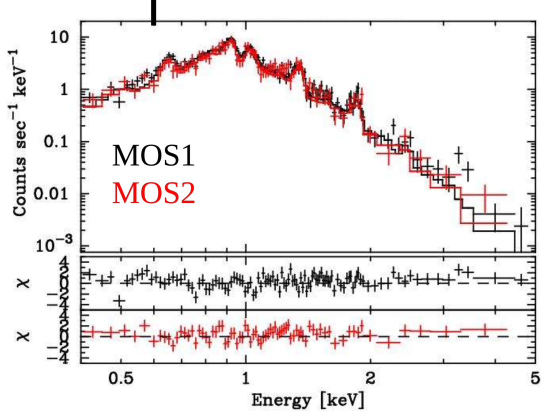

	East	North	West
kTe(keV):	0.32 ($^{+0.09}_{-0.08}$)	0.34 ($^{+0.03}_{-0.06}$)	0.31 ($^{+0.05}_{-0.03}$)
log(τ):	11.0 ($^{+0.33}_{-0.22}$)	10.9 ($^{+0.2}_{-0.1}$)	11.0 ($^{+0.15}_{-0.08}$)
O(=C=N):	0.10 ($^{+0.04}_{-0.02}$)	0.08 (+/-0.02)	0.08 ($^{+0.02}_{-0.01}$)
Ne:	0.23 ($^{+0.11}_{-0.06}$)	0.22 ($^{+0.04}_{-0.05}$)	0.20 ($^{+0.06}_{-0.02}$)
Mg:	0.19 ($^{+0.10}_{-0.06}$)	0.13 (+/-0.04)	0.09 ($^{+0.03}_{-0.02}$)
Si:	0.3 ($^{+0.23}_{-0.14}$)	0.28 ($^{+0.10}_{-0.09}$)	0.36 ($^{+0.11}_{-0.09}$)
S:	1 ($^{+1.0}_{-0.4}$)	1 ($^{+1.0}_{-0.6}$)	<0.75
Fe(=Ni):	0.12 ($^{+0.04}_{-0.03}$)	0.11 (+/-0.03)	0.10 ($^{+0.02}_{-0.01}$)

The rim region abundances are significantly low relative to solar values, which argues for a lack of ejecta contamination and points toward an interstellar medium (ISM) origin. Also, the abundance of Mg appears to decrease toward the west.

- Two-kTe component model fitting

Considering that both SN ejecta and swept-up ISM are present in Puppis A, we applied next a two-kTe component NEI model. In this model, kTe, t, and EM were allowed to be free parameters for each component. We fixed the metal abundances for the ISM component to those determined from the rim regions employing the depleted abundances found in our work. We left abundances of O(=C=N), Ne, Mg, Si, S, Fe(=Ni) for the ejecta component as free parameters.

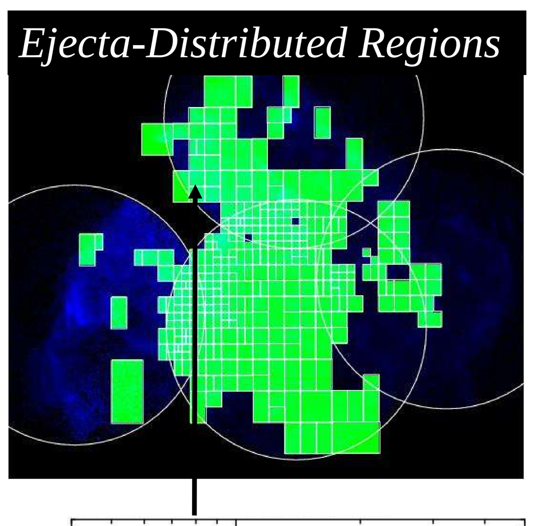

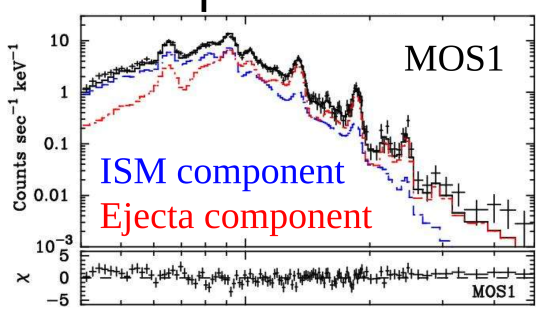

In this way, we fitted all spectra with the two-component NEI model. "Ejecta-distributed region" were defined as cells where these fits showed that (1) two components were required at high significance (> 99% from the F-test) and (2) the O abundance of the ejecta component was > 1 times the solar value. Cells satisfying these criteria are indicated as green regions overlaid on the X-ray surface brightness map in the figure at left. Example spectrum and the best-fit parameters are shown below. Maps of emission measures for all elements in the ejecta component are shown in the figures below, where lighter to darker color indicates more to less emission, respectively.

kTe(keV): 0.33 (+/-0.01); log(t): 11.17 (+/-0.07);

kTe(keV): 1.5 ($^{+0.11}_{-0.09}$); O: 6 (+/-1); log(τ): 10.4 (+/-0.04); Ne: 12 (+/-1); Mg: 15(+/-1); Si: 13(+/-1); S: 21(+/-5); Fe: 7(+/-)1

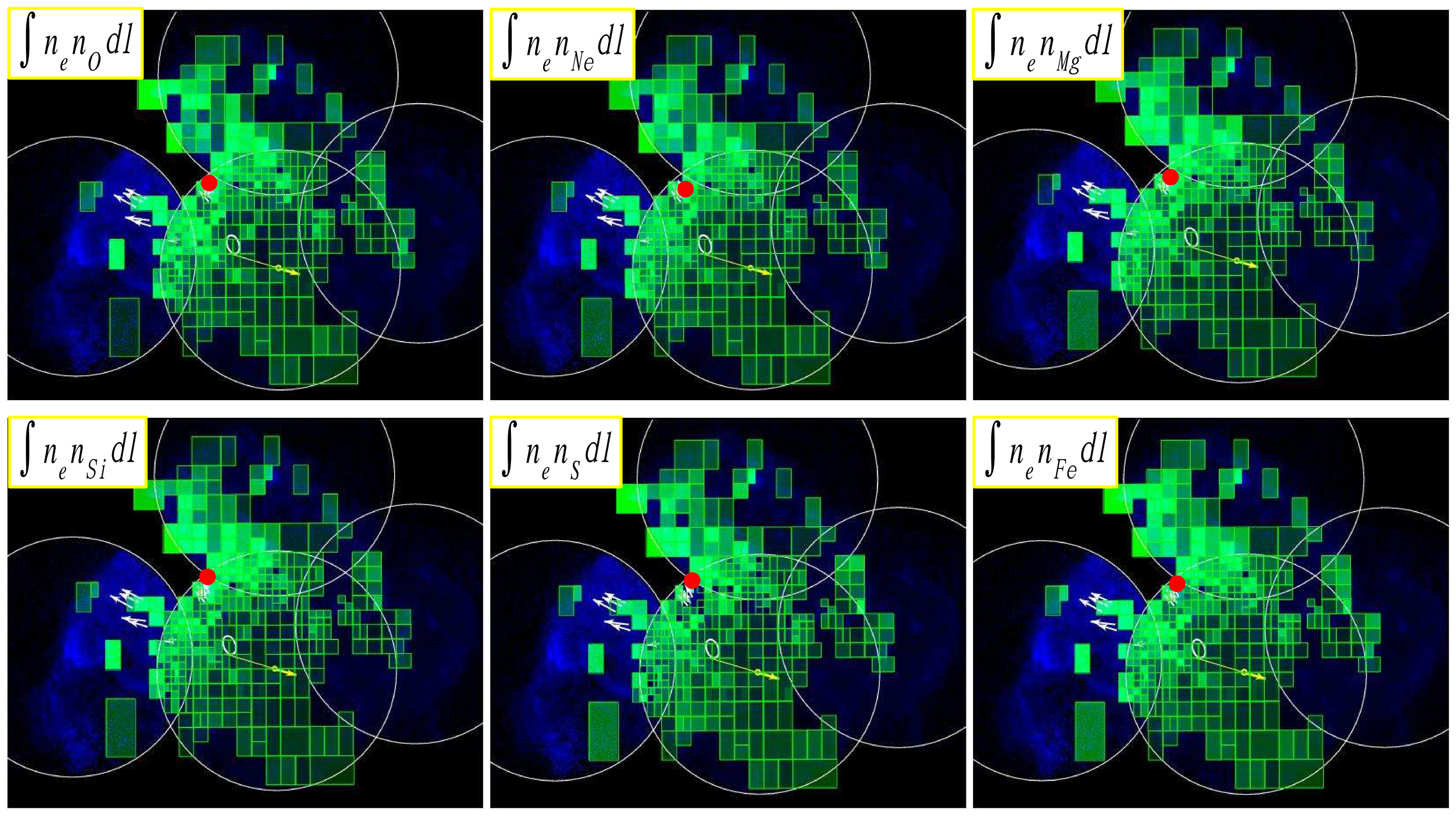

We find that the metals are all concentrated more toward the northeast than the southwest. We estimated emission integrals, EIs (EI=$\int n_e n_i dV$, dV is the X-ray-emitting volume) for all metals of the ejecta component in each cell and calculated the weighted mean location of all EIs which are shown as red filled circle in the above figures. In addition, the proper motion directions of the O-rich FMKs, the expansion center of the knots, and the proper motion direction of the compact remnant are also indicated as white arrows, a white ellipse, and a yellow arrow, respectively.

- Comparison with theoretical nucleosynthetic models

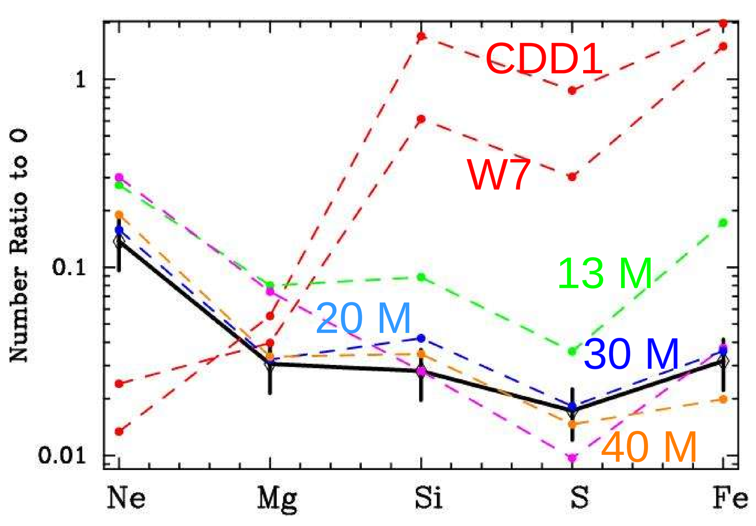

Black solid line represents our data. Note that the errors quoted are provisionally assumed to be ±30%.

We summed the EIs for O, Ne, Mg, Si, S, and Fe from the ejecta component over the entire remnant to obtain ~28, ~3.9, ~0.9, ~0.8, ~0.5, and ~0.9 x 10^{54} cm^{-3} in total, respectively. The figure at left compares our integrated measured abundances relative to O to theoretical nucleosynthetic yields (Iwamoto et al. 1999 for Type Ia; Tominaga 2007 for core-collapse). Our measured abundances are consistent with those expected from 30 and 40 M progenitor stars.

Summary

- We analyzed five XMM-Newton observations of Puppis A. The FOV covers almost the entire spatial extent of this remnant. Dividing the FOV into numerous small cells, we extracted spectra and performed spectral analysis on each cell using NEI models.

- A single temperature NEI model fairly well represents the data from the rim regions. The abundances obtained here are significantly low relative to the solar values, which is evidence that the ejecta contribution is negligible in the rims. We found a decrease of Mg abundance in rim regions toward the west of the remnant.

- Spectra from a large portion of the spatial extent of the remnant required an additional (i.e., ejecta) component in addition to the ISM one. We found that the metal-rich ejecta component was non-uniformly distributed, with the northeastern part of the remnant showing higher emission integrals than the southwestern. This is at least qualitatively consistent with the idea that the ejecta in Puppis A were ejected asymmetrically (more toward the northeast) while the CCO received a kick toward the southeast.

- The relative abundances of the ejecta component in the entire remnant were consistent with those expected from core-collapse SNe whose progenitor masses are 30 and 40 M.

References

Arendt, R. G., Dwek, E., Petre, R., Dickel, J. R., Roger, R. S., Milne, D. K., and Kesteven, M. J. 1990, ApJ, 350, 266
Aschenbach, B. 1993, Adv. Space Res., 13, 45
Blair, W. P., Sankrit, R., Ghavamian, P. Raymond, J. C., and Morse, J. A. 2003, AAS, 203, 3912B
Hui, C. Y., & Becker, W. 2006, A&A, 457L, 33
Iwamoto, K., Brachwitz, F., Nomoto, K., Kishimoto, N., Umeda, H., Hix, W. R., Thielemann, F-K. 1999, ApJS, 125, 439
Hwang U., Petre R., and Flanagan K. A. 2006, presentation given at "The Extreme Universe in the Suzaku Era"
Petre, R., Becker, C. M., & Winkler, P. F. 1996, ApJ, 456, L43
Scheck, L., Kifonidis, K., Janka, H.-Th, Muller, E. 2006, A&A, 457, 963
Tominaga 2007, in private communication.
Winkler, P. F. & Kirshner, R. P. 1985, ApJ, 299, 981
Winkler, P. F. & Petre, R. 2006, astro-ph/0608205